Rare-Earth Ions in the Alkali Halides. II. Pseudolocalized Vibrational Frequencies

MAX WAGNER* AND W. E. BRON
IBM Watson Research Center, Yorktown Heights, New York
(Received 22 October 1964; revised manuscript received 18 February 1965)

Vibronic structure observed in the emission and absorption spectra of alkali halides containing either Sm^{2+}, Eu^{2+}, or Yb^{2+} is reported, and shown to result from pseudolocalized vibrations occurring at the rare-earth defect. A model for the defect is defined, and an analysis of its vibrational frequencies is given for the sample case of a RbCl host lattice. A Green's function formalism is used in the analysis. The calculation, in which a number of approximations are made, yields the qualitative features of the experimental results.

INTRODUCTION

IN a recent paper[1] (number I in the series of papers on rare-earth ions in the alkali halides) an analysis was given of the crystal field splitting of the emission spectrum of the Sm^{2+} ion in a number of alkali-halide host lattices. The emission spectra consist of sets of very sharp lines which arise from electronic transitions between Stark components of states of the $4f^6$ ground configuration. In contrast, the absorption spectrum of Sm^{2+}, as well as the absorption and emission spectra of Eu^{2+} and Yb^{2+} in the alkali halides, consists of broad bands which arise most probably from transitions of the type $4f^n \rightleftarrows 4f^{n-1}5d$. Many of these broad bands show long series of sharp vibronic structure when measurements are made near liquid-helium temperatures. The vibrational frequency, obtained from the interval between successive lines of the vibronic series, overlaps the frequency region of lattice phonons. This indicates that the corresponding electronic levels of these ions are coupled to very narrow regions within the frequency band of the disturbed lattice, and we may suspect that these small spectral regions are just the regions where resonances occur in the phonon scattering, i.e., where there are pseudolocalized modes. Thus, these experiments provide a method to measure pseudolocalized modes without requiring that they have an electric dipole or that their frequency lie in a transparent region of the crystal. These latter restrictions are essential for the direct optical observation of local modes.[2]

On the other hand, the observation of these localized vibrations through vibronic spectra requires for their analysis not only an understanding of the pseudolocalized vibration, but also an understanding of the electron-lattice coupling. In the present paper we give an analysis of the pseudolocalized vibration, and in the paper immediately following this one (hereafter referred to as Ref. 3 and number III in the series of papers) we analyze the details of the vibronic spectra in terms of the electron-lattice dynamics.

The vibrations of a defect in a host lattice can be solved in principle by the Green's function formalism introduced by Lifshitz.[4] For practical calculations it becomes necessary to introduce certain approximations. The calculation of the pseudolocalized vibrations presented in the discussion of this paper is based on the simplest dynamical model which nevertheless yields all the qualitative features of the experimental results, and which can be used as a guide to a more complete calculation. For example, in practical calculations it is essential to know the Green's function of the lattice explicitly. For an idealized cubic lattice with nearest-neighbor central and noncentral force interactions, it has been tabulated extensively by Maradudin *et al.*,[5] but it is unknown for real crystals.

We shall establish, therefore, a Green's function by using suitable approximations, such as the adoption of the frequency-distribution curves of Karo[6] for alkali halide crystals. These distributions, which have been calculated by an improved Kellerman[7] procedure, have been proven to be in quite good agreement with experimental results. So we can hope to get a reasonable approximation for the Green's function of the real crystal.

Another essential restriction for the practical application of the Green's function formalism is that the number of lattice coordinates which are involved in the disturbance has to be small. This we shall do by assuming that the force constants are practically unchanged outside the immediate neighborhood of the center of disturbance. This seems to be an adequate assumption for all lattice points which have static displacements which are no greater than those involved in harmonic oscillations, and this is certainly true for the points outside the immediate neighborhood of the center, even if the center is not electrically neutral.

---

* Present address: Institut für theoretishe und angewandte Physik, Technishe Hochschule, Stuttgart, Germany.

[1] W. E. Bron and W. R. Heller, Phys. Rev. **136**, A1433 (1964).

[2] P. G. Dawber and R. J. Elliott, Proc. Roy. Soc. (London) **A273**, 222 (1963).

[3] W. E. Bron and M. Wagner, following paper, Phys. Rev. **139**, A233 (1965).

[4] I. M. Lifshitz, Nuovo Cimento Suppl. **3**, 716 (1956). This review article gives exhaustive reference to the original papers of Lifshitz.

[5] A. A. Maradudin, E. W. Montroll, G. H. Weiss, R. Herman, and H. W. Milnes, *Green's Functions for Monatomic Simple Cubic Lattices* (Academie Royale de Belgique, Memories XIV, 1960), Vol. 7.

[6] A. M. Karo, J. Chem. Phys. **31**, 1489 (1959); **33**, 7 (1960); J. R. Hardy, Phil. Mag. **4**, 1278 (1959); **7**, 315 (1960). J. R. Hardy and A. M. Karo, Phil. Mag. **5**, 859 (1960); Phys. Rev. **129**, 2024 (1963).

[7] E. W. Kellermann, Phil. Trans. Roy. Soc. London **238**, 513 (1940); Proc. Roy. Soc. (London) **A178**, 17 (1941).

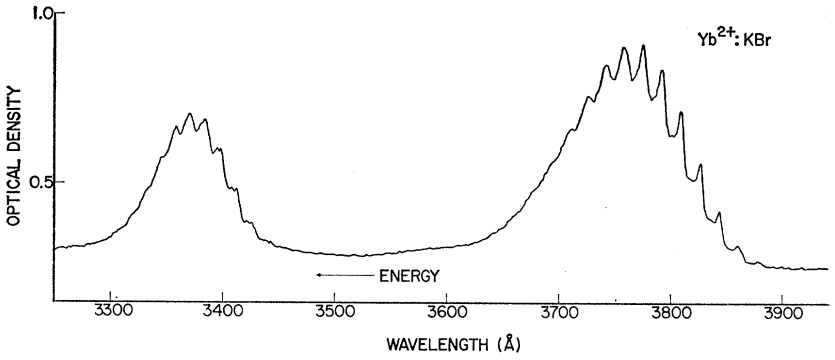

FIG. 1. The absorption spectrum of Yb^{2+}: KBr taken at 10°K showing the vibronic structure on the two lowest energy absorption bands.

EXPERIMENTAL METHODS

Single crystals of rare-earth-doped alkali halides were prepared by the Kyropoulos method from mixed melts of either $SmCl_2$, $EuCl_2$, or $YbCl_2$ in either NaCl, KCl, RbCl, KBr, or KI. As indicated in Ref. 1, all samples were quenched to room temperature from 600°C in order to remove rare-earth halide precipitates. The apparatus used to obtain the spectra is described in Ref. 1.

EXPERIMENTAL RESULTS

At room temperature the absorption spectra of Sm^{2+}, Eu^{2+}, and Yb^{2+} in the alkali halides consists of a number of broad bands. At 10°K these broad bands narrow somewhat, and their peak positions generally shift to somewhat lower energies. (For an example, see data for Sm^{2+}:KCl in Ref. 1.) In addition, at the lower temperature some of the broad bands have superimposed on them series of sharp vibronic lines with the interval between successive lines of any one series being essentially constant. For most of the samples studied, the vibronic structure was not observable at temperatures greater than about 30°K. The data presented here refers to measurements at about 10°K. In general, the vibronic structure occurs on the bands appearing in the low-energy part of an absorption spectrum. The lines are narrowest on the low-energy side of any one absorption band, and becomes progressively broader with increasing energy and are usually barely detectable on the high-energy side of the band. These general features of the absorption spectrum are illustrated in Fig. 1 for the case Yb^{2+}:KBr.

Similar vibronic structure appears on the emission bands of Eu^{2+} and Yb^{2+} in the alkali halides. For these ions two or more broad emission bands are observed, the lower energy one of which having the more pronounced sharp line structure. On the emission bands the lines are narrowest on the high-energy side, and become progressively broader with decreasing energy. See Fig. 2 for the case of the lowest energy emission band of Eu^{2+}:KI.

In general, each broad band has more than one series associated with it. The different series interweave, i.e., the first line of a second series occurs before the last line of a first series. As many as five distinct series have been observed on one broad band.

Usually any one vibronic series does not consist of a single set of equally spaced lines. Each major spacing contains a number of lines with a minor (smaller) interval which is again approximately constant. In what follows ω_1 is assigned to the frequency difference in the major interval, and ω_2 to that of the minor

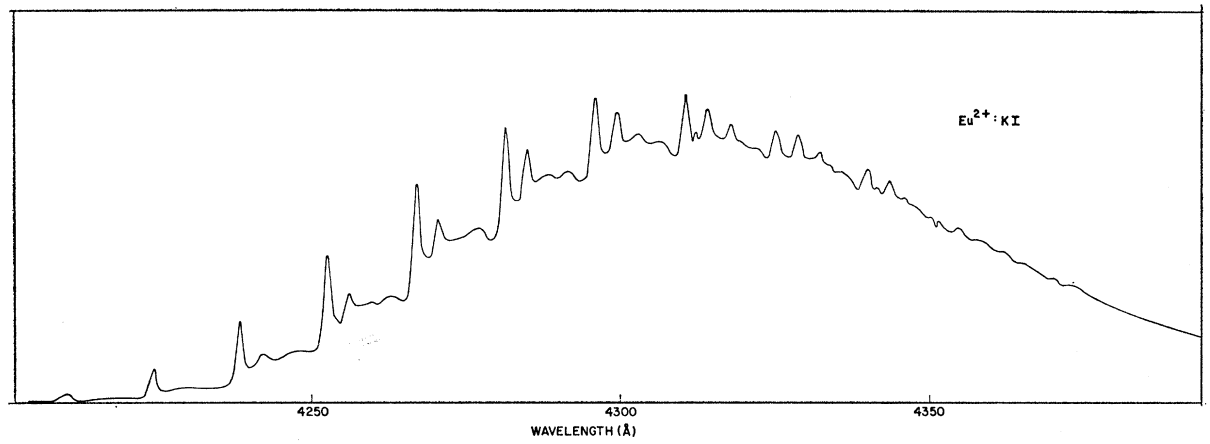

FIG. 2. Vibronic structure on the lowest energy emission band of Eu^{2+}: KI taken at 10°K.

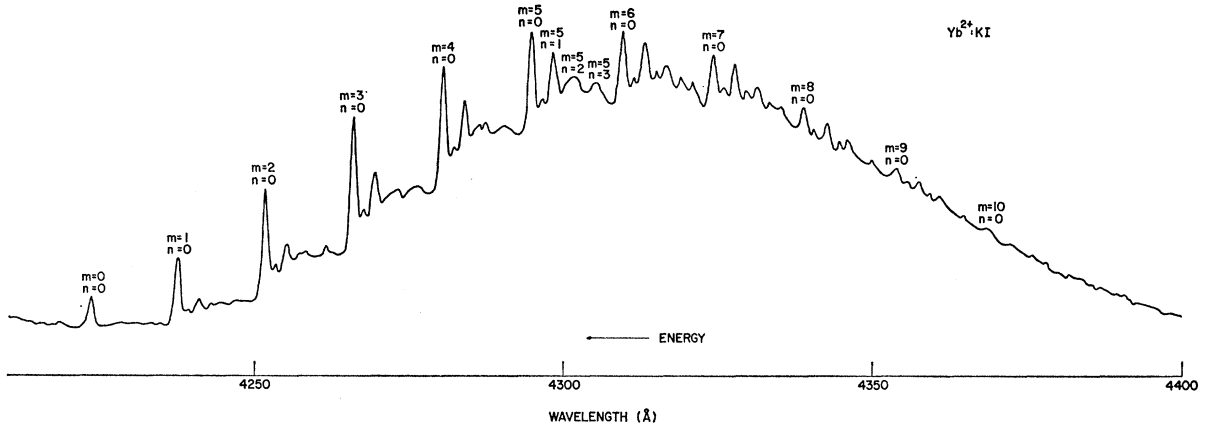

FIG. 3. Major and minor vibronic intervals observed on the lowest energy emission band of Yb^{2+}: KI at 10°K.

interval. Similarly, $m(0,1,2,3,\cdots)$ refers to an index which counts the lines of the major interval, and $n(0,1,2,3,\cdots)$ to that of the minor interval. Figure 3 illustrates such double vibronic frequency as observed in the emission spectrum of Yb^{2+}:KI. The minor interval is specifically enumerated for $m=5$, and is easily discernible for the other m values.

In the bromides and iodides ω_1 is small, and the number of vibronic lines in any one series is large, as compared to the chlorides. This can be seen from the examples of the data given in Table I for the lowest energy observed in the emission spectrum of Eu^{2+}:KI, and in Table II from similar data from Eu^{2+}:NaCl. This data also illustrates the general result that the frequency interval in any one vibronic series is essentially constant in the bromides and iodides, but has a slight monotonic decrease in the chlorides.[8] In the iodides and bromides ω_1 and ω_2 were determined by taking the average value of any one series, while in the chlorides the value of the first vibronic interval is reported. Table III lists ω_1 and ω_2 obtained in this way for the lowest energy absorption band and the lowest energy emission band of all samples investigated. The error in these values is of the order of ± 4 cm^{-1}. It should be noted from Table III that, with some exceptions, ω_1 and ω_2 for any one alkali halide is essentially independent of the rare-earth ion, and are only slightly higher in absorption than in emission. The vibronic frequencies decrease as either the cation or the anion of the alkali halide lattice becomes heavier, the dependence being much weaker on the next-nearest cation than on the nearest-neighbor anion mass. The anomalously high values of ω_1 (of the order of 800 cm^{-1}) observed in the absorption spectra of Eu^{2+}:NaCl, KCl, and RbCl correspond to the observed intervals between four sharp lines observed on the low-energy side of the lowest energy absorption band in each case. A comparison of the position of these lines with the spectra of Eu^{2+} in KBr and KI, as well as that in alkaline earth halides, appears to rule out the possibility that the sharp lines in the alkali chlorides arise from transitions to four pure electron states of the Eu^{2+} ion. Instead we have attributed these lines to a vibronic series whose vibrational interval has been increased as a result of a Jahn-Teller effect arising from the existence of an accidental degeneracy of two electronic states of the Eu^{2+} ion. We defer further discussion of this point to a forthcoming paper in which we give preliminary arguments for this interpretation.

TABLE I. Vibronic lines on lowest energy emission band of Eu^{2+}:KI.

m	λ (Å)	ν (cm^{-1})	$\Delta\nu$ (cm^{-1})
0	4210.5	23 750	
1	24.6	671	79
2	38.5	593	78
3	52.7	514	79
4	67.1	435	79
5	81.6	356	79
6	96.1	277	79
7	4310.5	199	78
8	25.3	120	79
9	40.0	041	79
10	55.5	22 962	79

[8] This monotonic decrease is real. The lines can be easily resolved from the broad background. For a discussion of the background see Ref. 3.

DISCUSSION

The vibronic frequencies ω_1 and ω_2 listed in Table III lie, with one exception, either in the optical or acoustical region of the lattice absorption[6] of the

TABLE II. Vibronic lines on lowest energy emission band of Eu^{2+}: NaCl.

m	λ (Å)	ν (cm^{-1})	$\Delta\nu$ (cm^{-1})
0	4224.0	23 674	
1	61.7	464	210
2	99.0	261	203
3	4332.8	080	181

TABLE III. Vibronic frequencies in rare-earth-doped alkali halides. Absorption (first excited state)

	NaCl		KCl		RbCl		KBr		KI	
	ω_1	ω_2	ω_1	ω_2	ω_1	ω_2	ω_1	ω_2	ω_1	ω_2
Sm^{2+}	215	52	208	23	193	27	115	39	85	56[b]
Eu^{2+}	794	54	822		831	36	116	37	86	24
Yb^{2+}	218		208	43	185		114		84	
Emission (ground state)										
Eu^{2+}	210	48	196	45	183	36	110	37	79	19
Yb^{2+}	208	45	203	44	183	42	108	37	79	19

[a] Frequencies given in cm^{-1}.
[b] Probably $2\omega_2$.

particular host. (The frequency in the 80 cm^{-1} region observed in KI actually falls in the gap between the optical and acoustical branches.) In general, therefore, the observed vibrations must be considered as pseudolocalized, since the frequencies occur in the pass band of lattice phonons.

The general formalism required for the analysis of pseudolocalized vibrations has been developed in detail elsewhere.[4,9,10] Our aim here is to apply this formalism to the vibrations of a divalent rare-earth ion in an alkali-halide lattice. We, therefore, outline only those results of the theory necessary to the calculation and for the definition of terms.

In Sec. I we discuss the approximations used to define those eigenvectors of the vibration of the undisturbed lattice which are required for the Green's function. The latter, as well as the eigenvalue equation for the pseudolocalized vibration, are given in Sec. II. Finally, in Sec. III we apply the formalism to an approximate model of the defect and solve for the eigenfrequencies.

I. Vibrations of the Ideal Lattice

The basic idea of the Green's function formalism is to reduce the high-dimensional problem to a low-dimensional one which includes only those lattice coordinates involved in the disturbance, whereas the influence of the other lattice coordinates is described by a Green's function given by the solutions of the undisturbed lattice. This necessitates that we know the latter.

The eigenvectors of the ideal lattice are well known to be of the plane-wave form[11]

$$\eta_{\nu\mathbf{n}}{}^{i}(\mathbf{k}\lambda)=N^{-3/2}\varepsilon_{\nu}{}^{i}(\mathbf{k}\lambda)\exp[i\mathbf{k}\cdot(\mathbf{n}+\mathbf{v})], \tag{1}$$

where $\mathbf{n}$ (or $\mathbf{m}$) is the position of a unit cell in the Bravais lattice, $\mathbf{v}$ (or $\mathfrak{y}$) is the position of the ions within the cell, $i(i=1, 2, 3)$ refers to the ith Cartesian component of η, and we have assumed that our lattice has N^3 unit cells. The lattice matrix in the harmonic approximation is real and symmetric, whence the eigenvectors can be chosen to constitute a complete orthonormal system. The $\mathbf{k}$ vectors define a reciprocal lattice with reduced spacing. The polarization vectors $\varepsilon_{\nu}{}^{i}(\mathbf{k}\lambda)$ are solutions of the $3s$-dimensional dynamical equation of the lattice, which gives also the $3s$ frequency branches $\omega(\mathbf{k}\lambda)$; ($s$=number of ions within the unit cell, $\lambda=1, \cdots, 3s$). The dynamical matrix $M_{\mu\nu}{}^{ij}(\mathbf{k})$ within this equation is given by a transformation of the original lattice matrix with the plane-wave part of (1). We refer to the standard literature for a more complete discussion.[12]

For a "general" $\mathbf{k}$ vector, i.e., for one which cannot be transformed into itself by any point-group operation of the reciprocal lattice (except by the unit operation), all $3s$ frequencies $\omega(\mathbf{k}\lambda)$ are different. If the $\mathbf{k}$ vector lies on an axis or a plane of symmetry, some solutions of $M_{\mu\nu}{}^{ij}(\mathbf{k})$ may be degenerate.[13] As the number of general $\mathbf{k}$ vectors is much larger than that of those which lie on symmetry axis or planes, one should expect that the case where all $3s$ frequencies of $M_{\mu\nu}{}^{ij}(\mathbf{k})$ are not degenerate will be predominant.

This statement is correct in principle. But for most ionic crystals we often have a quasidegeneracy, especially if the first Brillouin zone approaches a sphere. Then one has to a good approximation s nondegenerate longitudinal and s doubly degenerate transverse branches. This approaches a continuous $\mathbf{k}$ space, where $C_{\infty v}$ is the "group of $\mathbf{k}$," whence $\varepsilon_{\mu}(\mathbf{k}\lambda)$ must belong to the A_1 or E_1 representation. For the alkali halides the first Brillouin zone is a truncated octahedron and there this approximation is rather good, as shown by the detailed investigation of Kellerman.[7] Therefore, we can write the polarization vectors as:

$$\varepsilon_{\mu}(\mathbf{k}\lambda)=a_{\mu}(\mathbf{k}\lambda)\{\cos\phi\sin\theta,\ \sin\phi\sin\theta,\ \cos\theta\}] \text{ longitudinal waves} \tag{2}$$

$$\left.\begin{aligned}\varepsilon_{\mu}(\mathbf{k}\lambda)&=a_{\mu}(\mathbf{k}\lambda)\{\sin\phi,\ -\cos\phi,\ 0\}\\ \varepsilon_{\mu}(\mathbf{k}\lambda)&=a_{\mu}(\mathbf{k}\lambda)\{-\cos\phi\cos\theta,\ -\sin\phi\cos\theta,\ \sin\theta\}\end{aligned}\right\}\text{ transversal waves}, \tag{3}$$

where $a_{\mu}(\mathbf{k}\lambda)$ are polarization amplitudes, and k, θ, ϕ are the spherical coordinates in $\mathbf{k}$ space. For ionic crystals with inversion symmetry the dynamical matrix $M_{\mu\nu}{}^{ij}(\mathbf{k})$ is real and symmetric. This is especially true for an alkali-halide crystal, as shown by Kellerman,[7] but also for alkaline-earth-halide crystals, as shown

[9] M. V. Klein, Phys. Rev. **131**, 1500 (1963).
[10] M. Wagner, Phys. Rev. **133**, A750 (1964).
[11] G. Leibfried, *Handbuch der Physik*, edited by S. Flügge (Springer-Verlag, Berlin, 1955), Vol. 7, pp. 1, 145.
[12] M. Born, *Atomtheorie des festen Zustandes* (Verlag Julius Springer, Leipzig and Berlin, 1923), Vol. 2; M. Born and K. Huang, *Dynamical Theory of Crystal Lattices* (Clarendon Press, Oxford, England, 1956).
[13] J. C. Phillips, Phys. Rev. **104**, 1263 (1956).

recently by Ganesan and Srinivasan.[14] Then the polarization vectors $\varepsilon_\mu{}^i(\mathbf{k}\lambda)$ may be chosen real, normalized and orthogonal

$$\sum_{\mu i} \varepsilon_\mu{}^i(\mathbf{k}\lambda)\varepsilon_\mu{}^i(\mathbf{k}\lambda') = \delta_{\lambda\lambda'} \tag{4a}$$

or vice versa

$$\sum_\lambda \varepsilon_\mu{}^i(\mathbf{k}\lambda)\varepsilon_{\mu'}{}^{i'}(\mathbf{k}\lambda) = \delta_{\mu\mu'}\delta_{ii'}. \tag{4b}$$

The polarization vectors (2) and (3) are already chosen to be orthogonal and the normalization (4a) requires for a diatomic crystal that

$$[a_+(\mathbf{k}\lambda)]^2 + [a_-(\mathbf{k}\lambda)]^2 = 1 \tag{5}$$

by means of which all information about the vibrations of the ideal lattice is contained in two real scalar functions,

$$\omega(\mathbf{k}\lambda) \quad \text{and} \quad c(\mathbf{k}\lambda) = a_-(\mathbf{k}\lambda)/a_+(\mathbf{k}\lambda). \tag{6}$$

Here we have substituted + or − for $\mathfrak{y}$ to stand, respectively, for the amplitude at the alkali or the halide ion. However, both functions are not independent from one another. In view of the fact that for diatomic crystals each of the three branches, Equations (2) and (3), have both an optical frequency $\omega_{\mathrm{op}}(\mathbf{k}\lambda)$ and an acoustical one, $\omega_{\mathrm{ac}}(\mathbf{k}\lambda)$, where λ is one of the three branches (1 longitudinal, 2 transversal), one has

$$[a_+{}^{(\lambda)}]_{\mathrm{ac}}{}^2 = \frac{M_+\omega_{\mathrm{op}}{}^2(\mathbf{k}\lambda) - M_-\omega_{\mathrm{ac}}{}^2(\mathbf{k}\lambda)}{(M_+ + M_-)(\omega_{\mathrm{op}}{}^2 - \omega_{\mathrm{ac}}{}^2)}, \tag{7a}$$

$$[a_-{}^{(\lambda)}]_{\mathrm{op}}{}^2 = \frac{M_-\omega_{\mathrm{op}}{}^2(\mathbf{k}\lambda) - M_+\omega_{\mathrm{ac}}{}^2(\mathbf{k}\lambda)}{(M_+ + M_-)(\omega_{\mathrm{op}}{}^2 - \omega_{\mathrm{ac}}{}^2)} \tag{7b}$$

for the case $M_+ > M_-$.

II. Green's Function Formalism

If the lattice is disturbed the translational invariance breaks down and there is no longer the possibility of defining the eigenvectors by the points in the reciprocal lattice. The eigenvalue equation of the disturbed lattice, normalized to the ideal lattice masses M_μ, can be written in the form

$$[L - \omega_s{}^2 I]z(s) = -V(\omega_s)z(s) \tag{8}$$

where L is the matrix of the mass normalized force constants of the undisturbed lattice, I the unit matrix, and the disturbance matrix $V(\omega)$ is given by

$$V_{\mu\nu,\mathrm{mn}}{}^{ij}(\omega) = (M_\mu M_\nu)^{-1/2} H^{(1)}{}_{\mu\nu,\mathrm{mn}}{}^{ij} - \frac{M_{\mathrm{m}}{}^\mu - M_\mu}{M_\mu}\omega^2\delta_{\mathrm{mn}}\delta_{\mu\nu}\delta_{ij}, \tag{9}$$

$H^{(1)}$ being the disturbance in the force constants in terms of Cartesian coordinates and $M_{\mathrm{m}}{}^\mu$ the new lattice masses. It is to be emphasized that the new eigenvectors $z(s)$ are no longer orthogonal as were the corresponding vectors $\eta(\mathbf{k}\lambda)$ in the undisturbed lattice; this is because the $z(s)$ are normalized to the masses of the undisturbed lattice and therefore

$$\sum_{m\mu i}(M_{\mathrm{m}}{}^\mu/M_\mu) z_{\mu\mathrm{m}}{}^i(s)^* z_{\mu\mathrm{m}}{}^i(s') = \delta_{ss'} \tag{10a}$$

and

$$\sum_s (M_{\mathrm{m}}{}^\mu/M_\mu)^{1/2} z_{\mu\mathrm{m}}{}^i(s)^* (M_{\mathrm{n}}{}^\nu/M_\nu)^{1/2} z_{\nu n}{}^j(s) = \delta_{\mathrm{mn}}\delta_{\mu\nu}\delta_{ij}. \tag{10b}$$

This modification of the orthogonality relations becomes very important, if $z(s)$ is strongly localized around a region where the lattice masses $M_{\mathrm{m}}{}^\mu$ differ from the ideal ones.

The true eigenvectors are the orthonormal quantities

$$\zeta_{\mu\mathrm{m}}{}^i(s) = (M_{\mathrm{m}}{}^\mu/M_\mu)^{1/2} z_{\mu\mathrm{m}}{}^i(s). \tag{11}$$

A Green's function may be used to transform Eq. (8) to an integral equation form

$$z(s) = -G(\omega_s)V(\omega_s)z(s) \tag{12}$$

where the required Green's function is given by[9,10]

$$G_{\mu\nu,\mathrm{mn}}{}^{ij}(\omega) = \sum_{\mathbf{k}\lambda} \frac{\eta_{\mu\mathrm{m}}{}^i(\mathbf{k}\lambda)\eta_{\nu\mathrm{m}}{}^j(\mathbf{k}\lambda)}{\omega^2(\mathbf{k}\lambda) - \omega^2}. \tag{13}$$

This transformation reveals the advantage of the Green's function method, if we bear in mind that the disturbance $V(\omega)$ extends only over small regions of the crystal and is defined, therefore, by a low-rank matrix $v(\omega)$. The frequencies of the disturbed lattice are then given by the determinental equation

$$\det[I + g(\omega_s)v(\omega_s)] = 0. \tag{14}$$

This equation was first established and investigated by Lifshitz[4] and subsequently in the work of Montroll and Potts,[15] and many others. For a more detailed description of the Green's function method we refer to the article of Klein[9] and also to the book of Montroll *et al.*[16]

For pseudolocalized vibrations, for which the localized frequency is in the region of lattice frequencies $\omega(\mathbf{k}\lambda)$, the Green's function (13) is no longer defined, being an improper integral. We redefine it according to standard scattering theory as

$$G^+(\omega^2) = \sum_{\mathbf{k}\lambda} \frac{\eta(\mathbf{k}\lambda)\eta(\mathbf{k}\lambda)^*}{\omega^2(\mathbf{k}\lambda) - (\omega^2 + i\epsilon)} \tag{15}$$

which is the Green's function for the "outgoing" (or +)

[14] S. Ganesan and R. Srinivasan, Can. J. Phys. **40**, 74 (1962).

[15] E. W. Montroll and R. B. Potts, Phys. Rev. **100**, 525 (1955); **102**, 72 (1956). A. A. Maradudin, P. Mazur, E. W. Montroll, and G. H. Weiss, Rev. Mod. Phys. **30**, 175 (1958).

[16] A. A. Maradudin, E. W. Montroll, and G. H. Weiss, "Theory of Lattice Dynamics in the Harmonic Approximation," in *Solid State Physics*, edited by F. G. Seitz and D. Turnbull (Academic Press Inc., New York, 1963), Suppl.

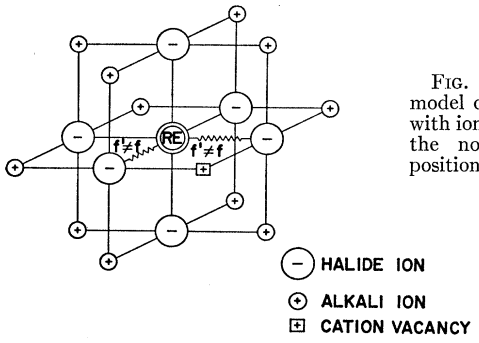

FIG. 4. Simplified model of the defect, with ions replaced at the normal lattice positions.

wave solution.[17] (ϵ is an infinitesimal positive number which we take to be zero after the calculation is performed.)

The eigenvalue equation now becomes

$$g^{+}ve(j)=\mu_j{}^{+}e(j) \tag{16}$$

where recognition has been given to the fact that the disturbance matrix V is of low rank v, and the $e(j)$ are a suitable set of normalized eigenvectors.

We indicate the connection to the scattering formalism by subdividing the total eigenvectors of the vibration into

$$Z(\mathbf{k}\lambda)=\eta(\mathbf{k}\lambda)+w(\mathbf{k}\lambda) \tag{17}$$

where we may consider $\eta(\mathbf{k}\lambda)$ as the incident phonon and $w(\mathbf{k}\lambda)$ as the scattering amplitude.

It is possible to write down a remarkably simple form for those components of the total eigenvector $Z^{+}(\mathbf{k}\lambda)$, which lie in the space of v,

$$Z^{+}(\mathbf{k}\lambda)=\sum_j \frac{\langle e(j)|\eta(\mathbf{k}\lambda)\rangle}{1+\mu_j{}^{+}}e(j). \tag{18}$$

Qualitatively speaking, the local amplitude can be very large if $|1+\mu_j|$ is very small, for which case the local amplitude may well exceed the nonlocalized one. As far as phonon scattering is concerned, this means a strong scattering. The strongest localized amplitude occurs if

$$1+R_e\mu_j{}^{+}(\omega)=0 \tag{19}$$

which is just the condition for a scattering resonance, if simultaneously the imaginary part of $\mu_j{}^{+}$, $\mathrm{Im}\mu_j{}^{+}$, is small.

For a detailed discussion of the scattering formalism, as applied to lattice vibrations, we refer the reader to the papers by Klein[9] and Wagner.[10]

III. Model of a Rare-Earth Defect in Alkali Halide Crystals

The defect responsible for the optical spectra observed in the alkali halides containing Sm^{2+} has been defined in some detail in Ref. 1. A positive ion vacancy, required for charge compensation, is present as a nearest 110 neighbor to the divalent cation impurity. In addition, static displacements of ions from normal lattice positions occur in the vicinity of the impurity ion. The largest static displacements are thought to be those of the divalent impurity and the center of charge of the vacancy toward each other. Because of the similarity in charge, size, and electronic configuration of Sm^{2+}, Eu^{2+}, and Yb^{2+}, it is reasonable to assume that the general features of the defect are the same for these rare-earth ions.

In order to simplify the calculation, as well as the interpretation, we assume that the only spring constants which are changed are the ones to the two nearest neighbors in the (100) and (010) direction. This is shown in Fig. 4.[18] The argument for this choice as a first step is that the rare-earth ion, of mass M_0, is statically displaced in the (110) direction which reduces the distance to the (100) and (010) ion, respectively, thus involving the non-Coulombic repulsion of the ionic cores. This should increase the spring constants to a much greater extent than the decrease of the springs in $(-1, 0, 0)$ and $(0, -1, 0)$ directions. Naturally this picture is oversimplified, but we shall use the calculation of this model as a guide to a more realistic choice. It is seen from Fig. 4 that only five coordinates are involved:

$$X=(X_0,Y_0,Z_0,X_1,Y_2). \tag{20}$$

They define a representation of $C_{2v}(110)$ and can be reduced to the following symmetry coordinates:

$$A_1\colon\ \frac{1}{\sqrt{2}}(X_0+Y_0),\ \frac{1}{\sqrt{2}}(X_1+Y_2), \tag{21a}$$

$$A_2\colon\ \text{none}, \tag{21b}$$

$$B_1\colon\ \frac{1}{\sqrt{2}}(X_0-Y_0),\ \frac{1}{\sqrt{2}}(X_1-Y_2), \tag{21c}$$

$$B_2\colon\ Z_0, \tag{21d}$$

where B_1 is defined in such a way that the basic functions are symmetric to the plane $\sigma_1=\sigma(x,y)$ and antisymmetric to $\sigma_2=\sigma(110,z)$, whereas the basic func-

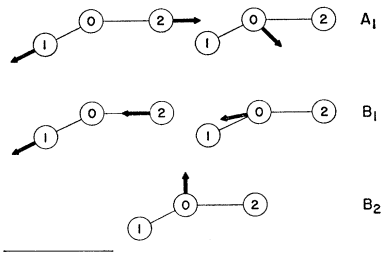

FIG. 5. Symmetry coordinates for the chosen model of the defect.

[17] See, for example, E. Merzbacher, *Quantum Mechanics* (John Wiley & Sons, Inc., New York, 1962), pp. 223, 490.

[18] In this figure we have, for the sake of clarity, omitted the displacement of ions from their normal lattice position.

tions of B_2 have the interchanged symmetry properties with respect to σ_1, σ_2. Figure 5 shows the symmetry vectors corresponding to the system (21a–d).

As the representation of $C_{2v}(110)$, given by (20), decomposes into

$$D(x)=2A_1+2B_1+B_2 \tag{22}$$

we shall see in the following consideration that the solution of the vibrational problem reduces to the solution of two 2-dimensional (A_1 and B_1) and one 1-dimensional equation for the five possible frequency branches of the quasilocalized modes.

The potential V of Eq. (8) is most easily found by using the Hermitian form

$$\begin{aligned}&\tfrac{1}{2}\langle X|H^{(1)}|X\rangle\\&=\tfrac{1}{2}(f'-f)\{(Y_2-Y_0)^2+(X_1-X_0)^2\}\\&=\tfrac{1}{2}(f'-f)[Y_2^2+Y_0^2+X_1^2+X_0^2-2Y_2Y_0-2X_1X_0]\end{aligned} \tag{23}$$

which is the addition to the potential energy of the vibrational equation due to the change $(f'-f)$ in the force constants. Using (9) and mass-normalized coordinates

$$(x_0,y_0,z_0)=M_+^{1/2}(X_0,Y_0,Z_0)\,,$$
$$(x_1,y_2)=M_-^{1/2}(X_1,Y_2)\,,$$

we have

$$\begin{aligned}\langle z|V|z\rangle&=(f'-f)\{M_-^{-1}y_2^2+M_+^{-1}y_0^2+M_-^{-1}x_1^2+M_+^{-1}x_0^2\\&\qquad-2(M_+M_-)^{-1/2}(y_2y_0+x_1x_0)\}-\omega^2\frac{M_0-M_+}{M_+}(x_0^2+y_0^2+z_0^2)\\&=(f'-f)\{M_-^{-1}(y_{A_1}^2+y_{B_1}^2)+M_+^{-1}(x_{A_1}^2+x_{B_1}^2)\\&\qquad-2(M_+M_-)^{-1/2}(x_{A_1}y_{A_1}+x_{B_1}y_{B_1})\}-\omega^2\frac{M_0-M_+}{M_+}(x_{A_1}^2+x_{B_1}^2+x_{B_2}^2)\end{aligned} \tag{24}$$

where, according to (21a–d)

$$x_{A_1}=\frac{1}{\sqrt{2}}(x_0+y_0)\,,\quad y_{A_1}=\frac{1}{\sqrt{2}}(x_1+y_2)\,, \tag{25a}$$

$$x_{B_1}=\frac{1}{\sqrt{2}}(x_0-y_0)\,,\quad y_{B_1}=\frac{1}{\sqrt{2}}(x_1-y_2)\,, \tag{25b}$$

$$x_{B_2}=z_0\,. \tag{25c}$$

Hence, the disturbance matrices become

$$V_{A_1}=V_{B_1}=\begin{pmatrix}(f'-f)/M_+-\omega^2(M_0-M_+)/M_+ & -(M_+M_-)^{-1/2}(f'-f)\\ -(M_+M_-)^{-1/2}(f'-f) & (f'-f)/M_-\end{pmatrix} \tag{26a}$$

$$V_{B_2}=-\omega^2\frac{M_0-M_+}{M_+} \tag{26b}$$

which has the obvious meaning that the 5×5 matrix V is decomposed into two 2×2 matrices (V_{A_1},V_{B_1}) and a scalar matrix V_{B_2}. The matrix g^+ can be decomposed in a similar way; we consider the scalar product

$$\begin{aligned}\langle z|g^+|z\rangle&=g_{00}{}^{11}x_0^2+g_{00}{}^{12}x_0y_0+g_{00}{}^{13}x_0z_0+g_{00}{}^{21}y_0x_0+g_{00}{}^{22}y_0^2+g_{00}{}^{23}y_0z_0+g_{00}{}^{31}z_0x_0+g_{00}{}^{32}z_0y_0+g_{00}{}^{33}z_0^2+(g_{01}{}^{11}+g_{10}{}^{11})x_0x_1\\&\quad+(g_{02}{}^{22}+g_{20}{}^{22})y_0y_2+(g_{02}{}^{12}+g_{20}{}^{21})x_0y_2+(g_{01}{}^{21}+g_{10}{}^{12})y_0x_1+(g_{01}{}^{31}+g_{10}{}^{23})z_0x_1\\&\quad+(g_{02}{}^{32}+g_{20}{}^{23})z_0y_2+g_{11}{}^{11}x_1^2+g_{22}{}^{22}y_2^2+(g_{12}{}^{12}+g_{21}{}^{21})x_1y_2\,,\end{aligned} \tag{27}$$

where we have used the abbreviation

$$g_{00}{}^{ij}=G\begin{matrix}\overset{i}{+}\\ 000,\end{matrix}\begin{matrix}\overset{j}{+}\\ 000\end{matrix}\,,\quad g_{01}{}^{ij}=G\begin{matrix}\overset{i}{+}\\ 000,\end{matrix}\begin{matrix}\overset{j}{-}\\ 000\end{matrix}\,,\ \text{etc.}\,, \tag{28}$$

where $\mathfrak{u}$ and $\mathfrak{v}$ are (+) for the rare-earth (R.E.) impurity located at the cation site at the origin, and are (−) for the nearest-neighbor halide ions. Expression (27) is readily transcribed into the symmetry coordinates (25a–c). $\langle z|g^{(+)}|z\rangle$ is invariant under the operations of the group $C_{2v}(110)$. Therefore, all terms with products of the coordinates of *different* irreducible representations must vanish, i.e., the coefficients of $x_{A_1}x_{B_1}$, $x_{A_1}x_{B_2}$, etc. By means of which we find the following properties:

$$g_{00}{}^{ij}=g_{0j}{}^{ij}=0\quad\text{for}\quad i\neq j\,. \tag{29}$$

Using the abbreviations

$$A=g_{00}{}^{11}=g_{00}{}^{22}=g_{00}{}^{33}=N^{-3}\sum_{\mathbf{k}\lambda}\frac{|\varepsilon_{+}{}^{x}(\mathbf{k}\lambda)|^2}{\omega^2(\mathbf{k}\lambda)-(\omega^2+i\epsilon)} \tag{30a}$$

$$B=g_{01}{}^{11}=g_{02}{}^{22}=N^{-3}\sum_{\mathbf{k}\lambda}\frac{\varepsilon_{+}{}^{x}(\mathbf{k}\lambda)\varepsilon_{-}{}^{y}(\mathbf{k}\lambda)}{\omega^2(\mathbf{k}\lambda)-(\omega^2+i\epsilon)}\exp(-iak_x) \tag{30b}$$

$$C=g_{11}{}^{11}=g_{22}{}^{22}=N^{-3}\sum_{\mathbf{k}\lambda}\frac{|\varepsilon_{-}{}^{x}(\mathbf{k}\lambda)|^2}{\omega^2(\mathbf{k}\lambda)-(\omega^2+i\epsilon)} \tag{30c}$$

$$D=g_{12}{}^{12}=N^{-3}\sum_{\mathbf{k}\lambda}\frac{\varepsilon_{-}{}^{x}(\mathbf{k}\lambda)\varepsilon_{-}{}^{y}(\mathbf{k}\lambda)}{\omega^2(\mathbf{k}\lambda)-(\omega^2+i\epsilon)}\exp[ia(k_x-k_y)], \tag{30d}$$

where a is the nearest-neighbor distance, k_i are the components of $\mathbf{k}$.

The scalar product $\langle z|g^{+}|z\rangle$ reduces to

$$\langle z|g^{+}|z\rangle=A(x_{A_1}{}^2+x_{B_1}{}^2)+Ax_{B_2}{}^2+2B(x_{A_1}y_{A_1}+x_{B_1}y_{B_1})+(C+D)(y_{A_1}{}^2+y_{B_1}{}^2) \tag{31}$$

or

$$g_{A_1}{}^{+}=g_{B_1}{}^{+}=\begin{pmatrix}A & B\\ B & (C+D)\end{pmatrix} \tag{32a}$$

$$g_{B_2}=A. \tag{32b}$$

Consequently,

$$g_{A_1}{}^{+}V_{A_1}=g_{B_1}{}^{+}V_{B_1}=\begin{pmatrix}A(\alpha-\omega^2\Delta)-\beta B & -\beta A+B\gamma\\ B(\alpha-\omega^2\Delta)-\beta(C+D) & -\beta B+(C+D)\gamma\end{pmatrix} \tag{33a}$$

$$g_{B_2}{}^{+}V_{B_2}=A\omega^2\Delta. \tag{33b}$$

We have used the abbreviations

$$\alpha=\frac{(f'-f)}{M_{+}},\quad \beta=(M_{+}M_{-})^{-1/2}(f'-f),\quad \gamma=\frac{(f'-f)}{M_{-}} \tag{34a}$$

$$\Delta=\frac{M_0-M_{+}}{M_{+}}, \tag{34b}$$

and we realize that

$$\alpha\gamma=\beta^2.$$

It is now almost trivial to calculate the eigenvalues of Eq. (16), which in our case of C_{2v} symmetry are $\mu_{A_1}{}^{(+)}$, $\mu_{A_1}{}^{(-)}$, $\mu_{B_1}{}^{(+)}$, $\mu_{B_1}{}^{(-)}$, μ_{B_2}. Inserting (33a) we arrive at

$$\mu_{A_1}{}^2-[A(\alpha-\omega^2\Delta)-2\beta B+(C+D)\gamma]\mu_{A_1}-\gamma\omega^2\Delta[A(C+D)-B^2]=0 \tag{35}$$

and

$$\mu_{B_2}=-A\omega^2\Delta. \tag{36}$$

From (35)

$$\mu_{A_1}{}^{(\pm)}=\mu_{B_1}{}^{(\pm)}=\tfrac{1}{2}[A(\alpha-\omega^2\Delta)-2\beta B+\gamma(C+D)]\pm\tfrac{1}{2}\{[A(\alpha-\omega^2\Delta)-2\beta B+\gamma(C+D)]^2+4\gamma\omega^2\Delta[A(C+D)-B^2]\}^{1/2}. \tag{37}$$

The quantities B and D are much smaller than A, C. This is so for two reasons: (a) They contain an oscillating factor [$\exp(-ik_xa)$ or $\exp(iak_x-iak_y)$, respectively] which reduces the absolute value of the sum [see Eqs. (30b), and (30d)]. (b) The product $\varepsilon_x{}^{(+)}(\mathbf{k}\lambda)\times\varepsilon_x{}^{(-)}(\mathbf{k}\lambda)$ is of opposite sign for the optical and acoustical branches [see Eq. (7b)], whereas the product $\varepsilon_x{}^{(-)}(\mathbf{k}\lambda)\varepsilon_y{}^{(-)}(\mathbf{k}\lambda)$ partly cancels, if we sum over λ, because of the closure property (4b). B and D are exactly zero for a simple cubic lattice with nearest-neighbor forces[19]; in such a model the Green's function matrix is diagonal in i and j (i.e., the Cartesian components of the displacements of the lattice points). For other models G^{ij} will not be exactly diagonal, but we expect the nondiagonal terms to be much smaller than the diagonal ones. For a careful discussion of this point we refer to the paper by Klein.[9] Neglecting B and D, (37) may be written in the form

$$\mu_{A_1}{}^{(\pm)}=\mu_{B_1}{}^{(\pm)}\approx\frac{\Omega^2}{2}\left\{\left[\tau A+\tau^{-1}C-\frac{\omega^2}{\Omega^2}\Delta A\right]\pm\left[\left(\tau A+\tau^{-1}C-\frac{\omega^2}{\Omega^2}\Delta A\right)^2+4\tau^{-1}\frac{\omega^2}{\Omega^2}AC\right]\right\}^{1/2}, \tag{38}$$

where [see (34a,b)]:

$$\Omega^2=(M_{+}M_{-})^{-1/2}(f'-f),\quad \tau=\left(\frac{M_{-}}{M_{+}}\right)^{1/2},\quad \Delta=\frac{M_0-M_{+}}{M_{+}}. \tag{39}$$

[19] H. B. Rosenstock and G. F. Newell, J. Phys. Chem. **21**, 1607 (1953).

The approximation (38) will be used for the numerical evaluation of the quasilocalized modes of the defect.

The Green's functions A and C are easily evaluated for alkali-halide lattices because of the simple approximation for the ideal eigenvectors $\eta(\mathbf{k}\lambda)$ outlined in Sec. I. Using these approximations, which reasonably include also

$$\omega(\mathbf{k}\lambda)=\omega_\lambda(|\mathbf{k}|) \tag{40}$$

which follows again from the fact that the first Brillouin zone for alkali-halide lattices is almost a sphere, and integrating Eq. (15) rather than summing up, we have

$$A_\lambda(\omega)=\int \frac{[a_+^{(\lambda)}(\omega_\lambda)]^2\rho_\lambda(\omega_\lambda)d\omega_\lambda}{\omega_\lambda^2-(\omega^2+i\epsilon)} \times\frac{1}{4\pi}\int \sin\theta d\theta d\phi\cdot\begin{Bmatrix}\cos^2\theta\\ \frac{1}{2}\sin^2\theta\end{Bmatrix}, \tag{41a}$$

$$C_\lambda(\omega)=\int \frac{[a_+^{(\lambda)}(\omega_\lambda)]^2\rho_\lambda(\omega_\lambda)d\omega_\lambda}{\omega_\lambda^2-(\omega^2+i\epsilon)} \times\frac{1}{4\pi}\int \sin\theta d\theta d\phi\cdot\begin{Bmatrix}\cos^2\theta\\ \frac{1}{2}\sin^2\theta\end{Bmatrix}, \tag{41b}$$

where the upper function refers to the longitudinal branches, the lower one to the transversal ones, and $a_+^{(\lambda)}$, $a_-^{(\lambda)}$ are the amplitudes of the positive and negative ions as defined by (2), (3), (5), (6), and (7). For the integration we have made use of the fact that the spectrum of ideal and disturbed frequencies is discrete but very dense, so that we replace

$$N^{-3}\sum_k\cdots \quad\text{by}\quad \frac{v_a}{(2\pi)^3}\int\cdots d^3k,$$

where v_a is an elementary volume of the original lattice. The angular integration is trivial and by means of (5) we have

$$A_\lambda(\omega)=\tfrac{1}{3}\int \frac{[a_+^{(\lambda)}(\omega_\lambda)]^2\rho_\lambda(\omega_\lambda)d\omega_\lambda}{\omega_\lambda^2-(\omega^2+i\epsilon)} \tag{42a}$$

$$C_\lambda(\omega)=\tfrac{1}{3}\int \frac{\rho_\lambda(\omega_\lambda)d\omega_\lambda}{\omega_\lambda^2-(\omega^2+i\epsilon)}-A_\lambda(\omega) \tag{42b}$$

and naturally

$$A(\omega)=\textstyle\sum_\lambda A_\lambda(\omega),\quad C(\omega)=\sum_\lambda C_\lambda(\omega). \tag{43}$$

It is elementary to evaluate the integrals (42a) (42b), if we use properly chosen frequency distributions $\rho_\lambda(\omega)$ for the four vibrational branches. Finally, it should be noted that within (43) the transverse branches are to be counted twice.

We now carry out the calculation for the pseudo-localized frequencies for the sample case of a R.E.$^{2+}$ ion in RbCl. In the evaluation of (42a,b) a choice exists as to the values to be used for $\rho_\lambda(\omega)$ and $[a_+^\lambda]^2$. For

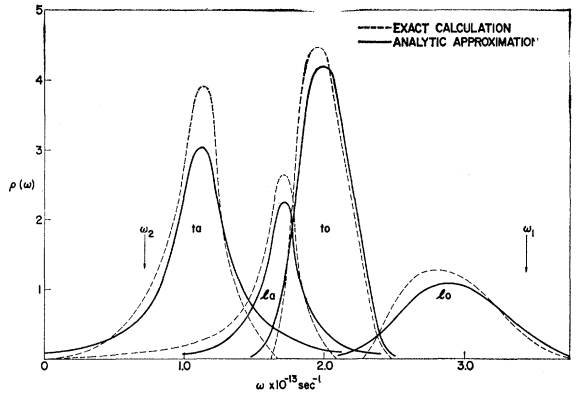

FIG. 6. Density of the vibrational states of the undisturbed RbCl lattice as calculated in Ref. 4 by A. M. Karo, and as approximated by Lorenzian analytic functions of Eqs. (4) and (5). The observed ω_1 and ω_2 frequencies are indicated by arrows.

$\rho_\lambda(\omega)$ it is possible to use a sum over a large representative number of eigenvectors available from the work of Karo.[6] We have chosen instead the integral form of (42a,b), and use for $\rho_\lambda(\omega)$ an analytical fit to the density-of-states curves calculated by Karo. This method is especially suitable for computer calculations, although it omits among other things the detailed effects of singular points in the phonon density of states.[20] Nevertheless, it may be considered a good first approximation to a more complete treatment since, as will be shown, it leads to reasonable results.

Accordingly, the frequency distribution has been approximated by

$$\rho_{\rm ac}{}^{(\omega)}=\frac{a/\pi}{(\omega-\omega_0{}^{(\lambda)})^2+a^2}, \tag{44a}$$

$$\rho_{\rm op}{}^{(\omega)}=\frac{b^3\sqrt{2}}{\omega_0{}^{(\lambda)}\pi}\,\frac{\omega}{(\omega-\omega_0{}^{(\lambda)})^4+b^4}. \tag{44b}$$

If $\lambda=1$, 2, 3, and 4 designate, respectively, the transverse-acoustical, the longitudinal-acoustical, the transverse-optical, and the longitudinal-optical branch, Eqs. (44a,b) can be fitted rather well to the distributions calculated by Karo[6] for RbCl with the following values (in units of 10^{+13} sec^{-1})

$$\omega_0{}^{\rm ta}=1.12,\quad \omega_0{}^{\rm la}=1.69,\quad \omega_0{}^{\rm to}=1.99,\quad \omega_0{}^{\rm lo}=2.88$$
$$a_{\rm ta}=0.21,\quad a_{\rm la}=0.14,\quad b_{\rm to}=0.22,\quad b_{\rm lo}=0.42.$$

[20] It has recently been shown [J. R. Hardy, Phys. Rev. **136**, A1745 (1964)] that the phonon spectrum of the undisturbed lattice may persist in lattices where the impurity concentration is very small. The selection rules for defect-activated lattice bands have recently been determined [R. London, Proc. Phys. Soc. (London) **84**, 379 (1964)] for simple defect configurations. The vibronic spectra reported in the present paper do not indicate any structure attributable to phonon states, although we have observed such vibronic structure in the spectra reported in Ref. 1. We defer for future investigation the question of the effect of phonon states, especially singular points, on the present vibronic structure.

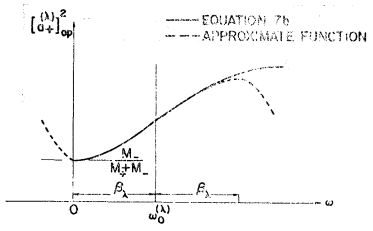

FIG. 7. Sketch of the comparison of $[a_+^{(\lambda)}]_{op}^2$ as given by Eqs. (7b) and (45).

These values have been chosen such that

$$\int_{-\infty}^{\infty}\rho_\lambda(\omega)d\omega=1$$

for the approximate distributions. In Fig. 6 the approximate distributions are compared to those calculated by Karo, which later have also been normalized to unity. For comparison, the position of the observed ω_1 and ω_2 frequencies are also shown in this figure.

An analytical function has also been used to approximate $[a_+^{(\lambda)}(\omega)]^2$

$$[a_+^{(\lambda)}(\omega)]^2=\gamma_\lambda+\alpha_\lambda\frac{(\omega-\omega_0^{(\lambda)})}{(\omega-\omega_0^{(\lambda)})^2+\beta_\lambda^2}, \qquad (45)$$

where α_λ, β_λ, and γ_λ are determined in such a manner as to fit the exact value of $[a_+^{(\lambda)}(\omega)]^2$ at $\omega=\omega_0^{(\lambda)}$, its first derivative at this point and to give the point $\omega=\omega_0^{(\lambda)}-\beta_\lambda$, the value $M_+/(M_++M_-)$ for the acoustical branches or the point $\omega=\omega_0^{(\lambda)}+\beta_\lambda$, the value $M_-/(M_++M_-)$ for the optical branches. We have sketched the function (45) in Fig. 7. The function (7a,b) cannot be exactly evaluated, although one may obtain the qualitative features of $[a_+^{(\lambda)}(\omega)]^2$ from the dispersion relationships given by Karo. It can be seen from Fig. 7 that the analytical fit (45) describes $[a_+^{(\lambda)}(\omega)]^2$ best near the $\omega_0^{(\lambda)}$, i.e., near the peak of the distributions $\rho_\lambda(\omega)$. But, since in the Green's function (42a,b) $[a_+^{(\lambda)}(\omega)]^2$ is weighted by the distribution $\rho_\lambda(\omega)$, the inconsistency in (45) far from the center of $\rho_\lambda(\omega)$ becomes unimportant.

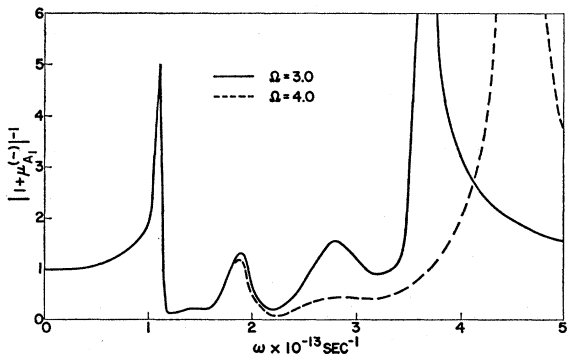

FIG. 8. The resonance denominator $|1+\mu_{A_1}{}^{(-)}|^{-1}$ as a function of the vibrational frequency ω as calculated for the two values of the force-constant parameter $\Omega=3$ and 4.

By means of these approximations $A(\omega)$, $C(\omega)$, $\mu_j(\omega)$ and, therefore, the resonance denominator $|1+\mu_j|^{-1}$ of Eq. (18) can be calculated. As will be shown in Ref. 3, only vibrational modes with A_1 symmetry can be coupled to electronic transitions for C_{2v} point symmetry. We therefore restrict the calculation to $\mu_{A_1}{}^{(\pm)}$. Of these, only $\mu_A{}^{(-)}$ yields solutions which satisfy condition (19).

The resonance denominator $|1+\mu_{A_1}{}^{(-)}|^{-1}$ has been calculated for various values of the force constant parameter Ω. In Fig. 8 the resultant values are plotted as a function of ω for $\Omega=3$ and 4. Two sharp resonances can be seen, one lying on the high-frequency side of the longitudinal-optical branch and the other near the peak of the transversal-acoustical branch of the undisturbed lattice. The higher frequency resonance depends on Ω, while the lower frequency does not. In order to discuss this result we would need to know the normal modes of vibration. To specify these in detail the eigenvectors of the vibration would need to be calculated, which in the present approximate calculation we have avoided doing. We can, however, construct a reasonable set of local normal vibrations of A_1 symmetry which have qualitatively the properties of the observed resonances by choosing linear combinations of the symmetry coordinates shown in Fig. 5 and given in Eq. (25a). These approximate normal modes are sketched in

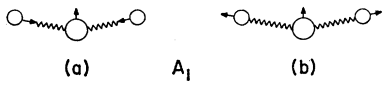

FIG. 9. Approximate normal local vibrations of A_1 symmetry.

Fig. 9. In the mode of Fig. 9(a), in which the motion of the R.E.$^{2+}$ ion and the halide ion are out of phase, these ions are forced against each other. The resultant vibrational frequency depends, therefore, on the local force constants as well as the masses of the ions. In the mode of Fig. 9(b), in which the motion of the ions is in phase, the vibrational frequency should be less sensitive to Ω, be a lower frequency than that of Fig. 9(a), but should be sensitive to the local masses.

The resonance frequency can be fitted to the ω_1 frequency with a value of Ω of approximately 2.75. However, since this is a one-parameter fit to the data, no great significance should be attached to this value. The low-frequency solution appears near 1.1×10^{13} sec^{-1} instead of the observed ω_2 of 0.73×10^{13} sec^{-1}. An attempt to improve this latter result, by substituting a Debye-Einstein distribution to fit exactly the low-frequency tails of the acoustical branches of the undisturbed lattice did not produce any substantial change in the result. This discrepancy is perhaps not too surprising in view of the approximation made in the calculation. Since the low-frequency A_1 mode is particularly sensitive to the effective mass of the rare-earth ion, one likely source of this error is the neglect of the effect of the positive-ion vacancy on the effective masses of the defect.

In conclusion, it has been shown that a crude calculation based on the Green's function formalism of pseudolocalized vibrations does yield two localized vibrational frequencies which have the qualitative features of the experimental results.

In the paper immediately following this one, we discuss the electron-lattice coupling, which we then use to analyze the details of the vibronic spectrum. Finally, we indicate how, in principle, the results of this analysis can be connected to the vibrational problem discussed in this paper. We defer, until the end of the next paper, a comparison of the results of the present vibronic spectra and those observed in other systems.

PHYSICAL REVIEW VOLUME 139, NUMBER 1A 5 JULY 1965

Rare-Earth Ions in the Alkali Halides. III. Electron-Lattice Coupling and the Details of the Vibronic Spectra

W. E. Bron and Max Wagner*
IBM Watson Research Center, Yorktown Heights, New York
(Received 22 October 1964; revised manuscript received 18 February 1965)

Electron-lattice interaction is discussed for the case of rare-earth ions in the alkali halides. A selection rule is derived to show that for the present defect electronic transitions can be coupled only to vibrational modes of A_1 symmetry. Under the assumption of electrostatic coupling between the electron and the lattice vibrations, a coupling function is derived which is proportional to the projection of the field of the electron undergoing a transition on to the eigenvectors of the vibrations. It is further shown that this coupling function can be determined from the details of the structural form of the vibronic spectra. A number of other features of the vibronic spectra are accounted for through the properties of Franck-Condon integrals.

INTRODUCTION

IN this paper, which is the third in the series on rare-earth ions in the alkali halides, we deal with the coupling of electronic transitions to the pseudolocalized lattice vibrations analyzed in the second paper in the series. [The first paper (marked I) has appeared previously[1] and the second (marked II) immediately precedes this one.[2]]

We show that selection rules exist which govern the coupling of electronic transitions to lattice vibrations. For the important case of an electrostatic coupling a more explicit discussion of the electron-lattice interaction is given. It is shown that for a center with inversion symmetry the coupling has no dipolar term; thus for ions whose electronic wave functions do not overlap the nearest lattice neighbors (e.g., rare-earth (R.E.) ions) the coupling can at best be quadrupolic. This restricted coupling makes it possible to obtain very sharp vibronic spectral lines. It also makes it possible to define a coupling function, which, in principle, can be obtained experimentally from the structural form of the vibronic line spectra. Finally, the details of the spectra are accounted for in terms of the properties of Franck-Condon integrals.

EXPERIMENTAL RESULTS

The experimental methods have already been described. We refer the reader to Refs. 1 and 2.

Many details of the vibronic spectra have already been given in Ref. 2. Figure 1 shows a representative vibronic spectra as observed on the lowest energy emission band in Yb^{2+}:KI at 10°K. This figure shows the general result, that any one vibronic series does not consist of a single set of equally spaced lines. Each major spacing contains a number of lines with a minor interval which is again approximately constant. Here, we adopt the notation given in Ref. 2, and assign ω_1 to the frequency difference in the major interval, and ω_2 to that of the minor interval. Similarly, $m(0,1,2,\cdots)$ refers to an index which counts the lines of the major interval and $n(0,1,2,\cdots)$ to that of the minor interval. The minor interval is specifically enumerated in Fig. 1 for $m=5$ and is easily discernible for other m values. This figure also shows the general result that the sharp-line vibronic spectra is found on the high-energy side of the broad emission bands. The converse is observed on absorption bands where the sharp vibronic lines are observed to be displaced asymmetrically against the low-energy side of the broad-band background.

Measurements have been made of the integrated intensities of the lines of the main (ω_1) vibronic series observed in the emission spectra of the Eu^{2+}-doped alkali halides. Table I lists the lines of the lowest energy

* Present address: Institut für Theoretische und Angewandte Physik der Technische Hochschule, Stuttgart, Germany.
[1] W. E. Bron and W. R. Heller, Phys. Rev. **136**, A1433 (1964).
[2] M. Wagner and W. E. Bron, preceding paper, Phys. Rev. **139**, A223 (1965).